Toxicology Reports 1 (2014) 459–473

Contents lists available at ScienceDirect

Toxicology Reports

journal homepage: www.elsevier.com/locate/toxrep

Mechanisms linked to differences in the mutagenic potential of 1,3-dinitropyrene and 1,8-dinitropyrene

J.A. Holme[a,*], H.E. Nyvold[a], V. Tat[b], V.M. Arlt[c], A. Bhargava[b], K.B. Gutzkow[a], A. Solhaug[d], M. Låg[a], R. Becher[a], P.E. Schwarze[a], K. Ask[b], L. Ekeren[a], J. Øvrevik[a]

[a] Division of Environmental Medicine, Norwegian Institute of Public Health, N-0403 Oslo, Norway
[b] Department of Medicine, McMaster University, Hamilton, ON, Canada
[c] Analytical and Environmental Sciences Division, MRC-PHE Centre for Environment and Health, King's College London, London, United Kingdom
[d] Norwegian Veterinary Institute, Oslo, Norway

ARTICLE INFO

Article history:
Received 26 March 2014
Received in revised form 7 July 2014
Accepted 8 July 2014
Available online 27 July 2014

Keywords:
Nitro-PAHs
1,3-Dinitropyrene
1,8-Dinitropyrene
DNA damage
Apoptosis

ABSTRACT

This study explores and characterizes the toxicity of two closely related carcinogenic dinitro-pyrenes (DNPs), 1,3-DNP and 1,8-DNP, in human bronchial epithelial BEAS-2B cells and mouse hepatoma Hepa1c1c7 cells. Neither 1,3-DNP nor 1,8-DNP (3–30 μM) induced cell death in BEAS-2B cells. In Hepa1c1c7 cells only 1,3-DNP (10–30 μM) induced a mixture of apoptotic and necrotic cell death after 24 h. Both compounds increased the level of reactive oxygen species (ROS) in BEAS-2B as measured by CM-H_2DCFDA-fluorescence. A corresponding increase in oxidative damage to DNA was revealed by the formamidopyrimidine-DNA glycosylase (fpg)-modified comet assay. Without fpg, DNP-induced DNA damage detected by the comet assay was only found in Hepa1c1c7 cells. Only 1,8-DNP formed DNA adduct measured by ^{32}P-postlabelling. In Hepa1c1c cells, 1,8-DNP induced phosphorylation of H2AX (γH2AX) and p53 at a lower concentration than 1,3-DNP and there was no direct correlation between DNA damage/DNA damage response (DR) and induced cytotoxicity. On the other hand, 1,3-DNP-induced apoptosis was inhibited by pifithrin-α, an inhibitor of p53 transcriptional activity. Furthermore, 1,3-DNP triggered an unfolded protein response (UPR), as measured by an increased expression of CHOP, ATF4 and XBP1. Thus, other types of damage possibly linked to endoplasmic reticulum (ER)-stress and/or UPR could be involved in the induced apoptosis. Our results suggest that the stronger carcinogenic potency of 1,8-DNP compared to 1,3-DNP is linked to its higher genotoxic effects. This in combination with its lower potency to induce cell death may increase the probability of causing mutations.

Abbreviations: AhR, aromatic hydrocarbon receptor; B[*a*]P, benzo[a]pyrene; Chk, checkpoint kinases; CYP, cytochrome P450; DMSO, dimethyl sulfoxide; DHE, dihydroethidium; 1,3-DNP, 1,3-dinitropyrene; 1,8-DNP, 1,8-dinitropyrene; DDR, DNA damage response; ER, endoplasmic reticulum; fpg, formamidopyrimidine-DNA glycosylase; Hoechst 33342, 2′-(4-ethoxyphenyl)-2′,5′-bis-1H-benzimidazole hydrochloride); γH2AX, phosphorylated H2AX; CM-H2DCFDA or H2DCFDA, 5-(and 6-)chloromethyl-2,7-dichlorodihydrofluorescein diacetate; Hoechst 33258, 2(2-(4-hydroxyphenyl)-6-benzimidazole-6-(1-methyl-4-piperazyl)benzimidazole hydrochloride); 1-NP, 1-nitropyrene; 3-NBA, 3-nitrobenzanthrone; RNS, reactive nitrogen species; NR, nitro-reductasesnitro-PAHnitro substituted-polycyclic aromatic hydrocarbon; PM, particular matter; PAH, polycyclic aromatic hydrocarbon; PARP, poly(ADP-ribose) polymerase; PI, propidium iodide; PFT, pifithrin; ROS, reactive oxygen species; SSB, single strand breaks; UPR, unfolded protein response; zVAD-FMK, benzyolcarbonayl-Val-Ala-Asp-fluoromethyl ketone.

* Corresponding author at: Department of Air Pollution and Noise, Division of Environmental Medicine, Norwegian Institute of Public Health, P.O. Box 4404, Nydalen, N-0403 Oslo, Norway. Tel.: +47 21076247; fax: +47 21076686.
E-mail address: jorn.holme@fhi.no (J.A. Holme).

http://dx.doi.org/10.1016/j.toxrep.2014.07.009

1. Introduction

Epidemiological studies link exposure to urban air particular matter (PM) with an increased risk of lung cancer [1–3] and in October 2013 the International Agency for Research on Cancer (IARC) classified outdoor air pollution as carcinogenic to humans (Group 1). Urban air PM is a heterogeneous mixture of various type of PM including combustion particles like diesel exhaust PM. These particles contain polycyclic aromatic hydrocarbons (PAHs) and nitro-PAHs, formed during the incomplete combustion, which have been suggested to play an important role in the PM-induced carcinogenesis [4]. Experimental studies have shown that many PAHs and nitro-PAHs are highly mutagenic and can cause tumors in animal models [5,6].

Nitro-PAHs can be metabolized into corresponding arylhydroxyamines both by cytosolic nitro-reductases (NR) and microsomal cytochrome P450 (CYP) enzymes [7]. CYP enzymes can activate the PAH-ring to epoxide intermediates that can be further converted to more reactive diol-epoxides [8]. Arylhydroxyamines can be further activated by *N*-acetylation or sulfonation [1,9]. Reduction of nitro-PAHs to the corresponding amines may also lead to the production of reactive oxygen (ROS) or nitrogen (RNS) species depending on the nitro-reductase and the availability of oxygen [1,10,11]. Nitro-PAHs can induce cellular toxicity in many ways and besides DNA damage, lysosomal and mitochondrial damage have been suggested to be important triggering signals [12–15].

DNA damage triggers a complex protein kinase signaling cascade, the so-called DNA damage response (DDR), which can activate cell cycle checkpoint kinases (Chk1/2) thereby promoting DNA repair and/or trigger apoptosis [16,17]. The resulting DDR depends on the type of damage (DNA adducts as well as single- and double-strand breaks [SSB and DSB]) as well as amount of damage. H2AX is a DDR protein which is phosphorylated into γH2AX often following DSB [18,19]. The protein kinase ATM (ataxia telangiectasia mutated) and ATR (ATM and Rad3-related) regulates Chk1/2 signaling, resulting in phosphorylation and activation of p53 [20–22]. Increased phosphorylation of p53 may up-regulate expression of p21 leading to cell cycle arrest or the expression of cell surface receptors like Fas as well as mitochondrial pro-apoptotic proteins like Bax, Bak, PUMA and NOXA [23,24]. Thus p53 is central both with regard to regulating cell cycle arrest giving time for DNA repair or triggering death/apoptotic signaling pathways.

Endoplasmatic reticulum (ER) stress and the consequent unfolded protein response (UPR) are involved in various pathological conditions [25,26] and can be triggered by a variety of environmental factors including chemical pollutants [27–29]. Prolonged ER stress is sensed by the UPR pathway through three known ER membrane bound transducers: IRE1, ATF6 and PERK [25]. IRE1 may be directly activated by unfolded proteins while ATF6 and PERK require the release of the chaperone GRP78 which dissociates when unfolded proteins accumulate in the ER [30]. Markers of the UPR response includes increased expression of GRP78, CHOP, ATF6, ATF4, and XBP1. These pathways attenuate ER stress by promoting protein folding, inhibiting mRNA translation, and by facilitating degradation of unfolded proteins. However, if ER-stress is prolonged or too extensive the UPR may also trigger cell death. In particular ATF4 and its downstream target CHOP, a pro-apoptotic transcription factor, appears central in UPR-mediated cell death [30].

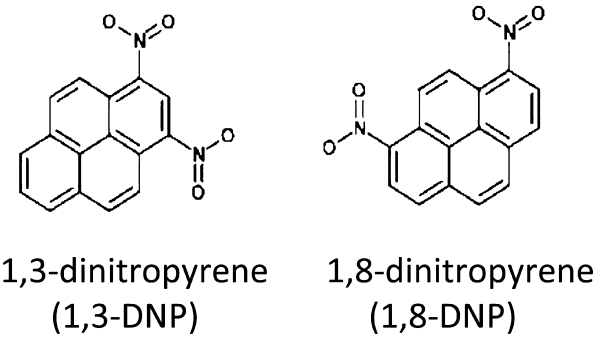

Fig. 1. Chemical structures of the test compounds.

Cell death has traditionally been classified into apoptosis or necrosis, but recent scientific advances have revealed a number of other modes of cell death including various forms of programmed necrosis, senescence, autophagy and mitotic catastrophe [31]. In previous studies we have successfully used the mouse hepatoma cell line Hepa1c1c7 as a model system to investigate various forms of cell death induced by PAHs and nitro-PAHs [14,32,33]. This cell line has a high aryl hydrocarbon receptor (AhR)-inducible capacity which promotes the metabolic activation of these compounds. One of the most important findings was that reactive metabolites may trigger different death signaling pathways as well as anti-apoptotic and pro-survival signals which are important determinants for the final outcome. Even closely related chemicals were found to trigger different types of cell death ([12,13,34]). This was also the case when using human bronchial epithelial BEAS-2B cells as an experimental model [35]. BEAS-2B cells are a commonly used model for studying the cytotoxicity and genotoxicity of air pollution components. In previous studies we have shown that urban air PM as well as several individual nitro-PAHs resulted in AhR-dependent CYP expression, DNA damage and a DDR resulting in apoptosis, and/or the release of cytokines [35–40].

In the present study we have compared various cytotoxic and genotoxic effects/responses of two closely related carcinogenic dinitro-pyrenes (DNPs) in the two cell models (Fig. 1). Both cell lines were exposed to 1,3-DNP and the more potent carcinogen 1,8-DNP [6,41,42]. Overall, BEAS-2B cells responded with the induction of ROS and oxidative damage to DNA, while Hepa1c1c7 cells seemed to be a more sensitive cellular model with regards to the formation of DNA adducts, DDR (1,8-DNP) and cell death (1,3-DNP). Our results suggest that the stronger carcinogenic potency of 1,8-DNP compared to 1,3-DNP is linked to its higher genotoxic effects. This in combination with its lower potency to induce cell death increases the probability of causing mutations.

2. Materials and methods

2.1. Chemicals

LHC-9 cell culture medium, 5-(and 6-) chloromethyl-2,7-dichlorodihydrofluorescein diacetate (CM-H_2DCFDA in short H_2DCFDA), dihydroethidium (DHE) were from Life Technologies (Carlsbad, CA, USA). Sterile HBS and purified collagen, PureCol™, were from Inamed Biomaterials (Freemont, CA, USA). 1,3-Dinitropyrene (1,3-DNP), 1,8-dinitropyrene (1,8-DNP), benzo[*a*]pyrene (B[*a*]P), bovine serum albumin (BSA), dimethyl sulfoxide (DMSO), ethylenediamineteraacetic acid (EDTA), Hoechst 33258, Hoechst 33342, aprotinin, Pifithrin-μ (PFT-μ), Ponceau S, phenylmethylsulfonyl fluoride (PMSF), propidium iodide (PI), polyoxyethylene octyl phenyl ether (Triton X-100) and zVAD-FMK were obtained from Sigma–Aldrich (St. Louis, MO, USA). Pifithrin-α (PFT-α) and Pepstatin A were from Calbiochem (Cambridge, CA, USA). Leupeptin was from Amersham Biosciences (Uppsala, Sweden). Bio-Rad DC protein assay was from Bio-Rad Laboratories, Inc (Hercules, CA, USA). Fetal calf serum (FCS), gentamycin, MEM alpha medium with L-glutamine, without ribonucleosides and deoxyribonucleosides were from Gibco BRL (Paisley, UK). UltraPure™ Low Melting-Point Agarose was purchased from Invitrogen (Paisley, UK). All other chemicals were of analytical grade and purchased from commercial sources.

2.2. Antibodies

Antibodies against cleaved caspase 3, phospho-p53 (Ser15), p53, cleaved PARP (Asp214), β-actin, phospho-H2AX (Ser139) were obtained from Cell Signaling (Beverly, MA, USA). NOXA was purchased from Santa Cruz Biotechnology, Inc, (Santa Cruz, CA, USA). As secondary antibodies horseradish peroxidase-conjugated goat-anti-rabbit (Sigma), horseradish peroxidase-conjugated rabbit anti-goat or rabbit anti-mouse IgG from Dako (Glostrup, Denmark) were used.

2.3. Cell culture

BEAS-2B cells, immortalized SV40-adenovirus-hybrid (Ad12SV40) transformed human bronchial epithelial cells, were purchased from the American Tissue Type Culture Collection (ATTCC, Rockville, MD, USA). In these cells p53 is mutated in codon 47, a sequence change that is reported not to change its functional properties [43,44]. Cells were grown in LHC-9 medium on collagen (PureCol™)-coated culture flasks and dishes. Cells were grown in 5% CO_2 humidified air at 37 °C and kept in a logarithmic growth phase ($1–9 \times 10^6$ cells/75 cm^2 flasks). Cells were split twice a week.

The mouse hepatoma Hepa1c1c7 cell line was purchased from the European Collection of Cell Culture (ECACC). Maintenance of the cells was done according to ECACC's guidelines and they were grown in alpha MEM medium with 2 mM L-glutamine, without ribonucleotides and deoxyribonucleotides. The media was supplemented with 10% heat-inactivated FCS and 0.1 mg/mL of the fungicide gentamycin. Cells were grown in 5% CO_2 humidified air at 37 °C and kept in a logarithmic growth phase ($1–9 \times 10^9$ cells/75 cm^2 flasks). Cells were split twice a week.

2.4. Exposure

BEAS-2B cells were plated in 35 mm 6-well dishes (8×10^4 or 10×10^4 cells/well). Fresh medium was added the day after seeding and right before exposure. Hepa1c1c7 cells were seeded in dishes (35 mm 6-well culture dishes or 90 mm culture dishes) or trays at a density of 70,000 cells per cm^2 the day before exposure. Fresh medium was added before exposure. When inhibitors were used, cells were pre-incubated with the inhibitor for 1 h before adding the test substances. Cells were treated with 1,3-DNP or 1,8-DNP. Cells treated with the solvent, DMSO, were used as controls. The amount of DMSO added to the culture medium was always less than 0.5%. B[*a*]P (15 μM) was included as positive control. After exposure cells were always briefly analyzed by light microscopy to verify any toxic response.

2.5. Fluorescence microscopy

To characterize cytotoxicity, the cells were exposed to test substance for 24 h and analyzed by fluorescence microscopy after staining with Hoechst 33342 (5 μg/mL) and PI (10 μg/mL), and prepared on a microscopy slide. Cell morphology was evaluated using a Nikon Eclipse E 400 fluorescent microscope, with an UV-2A excitation filter 330–380 nm (magnification 1000×). At least 300 cells were counted per slide and classified as either viable, apoptotic or necrotic. Cells with clearly condensed and/or fragmented nuclei (both PI-negative and PI-positive) as well as PI-negative cells with partial chromatin condensation were counted as apoptotic and determined as a fraction of the total number of cells. PI-stained cells exhibiting a rounded morphology and homogenously stained nucleus (typical necrotic) or partially condensed chromatin with less fluorescent intensities were termed PI positive. Non apoptotic cells, excluding PI, were considered as viable cells [12].

2.6. Flow cytometry

2.6.1. Cell cycle analysis

After treatment for 24 h, cells were trypsinated and prepared for flow cytometry. Cellular DNA was stained with Hoechst 33258 (1.0 μg/mL) and Triton X-100 (0.1%) and analyzed using the BD SLR II flow cytometer. Percentages of cells in the different phases of cell cycle were estimated using the Multicycle Program (Phoenix Flow System, San Diego, CA, USA) [45,46].

2.6.2. ROS measurements

ROS production was detected using flow cytometry and the oxidation-sensitive fluorescent probes CM-H_2DCFDA (1 μM) to detect hydrogen peroxide and DHE (5 μM) to detect superoxide anions [47]. Briefly, cells were loaded with CM-H_2DCFDA or DHE for the 2 last h of exposure to

test-substances for 2 or 24 h. After exposure, cells were washed twice with ice cold phosphate-buffered saline (PBS) and analyzed by flow cytometry to exclude ROS excreted from dead cells, and effects masked by any possibly reduction of cell proliferation. Pro-oxidants that were used as positive controls included incubation with 1 mM hydrogen peroxide for CM-H_2DCFDA and 100 μM menadione for DHE. The substances had some auto-fluorescence, but this did not affect the obtained results.

2.7. Single cell gel electrophoresis (comet assay)

The comet assay was performed as described previously [48]. Briefly, cells were exposed to 1,3-DNP, 1,8-DNP (1, 3, 10 or 30 μM) or B[*a*]P (10 μM) for 24 h. Media was removed and cells were trypsinated and re-suspended at 10^6 cells/mL in medium containing 10% FCS. Cells were dissolved in 0.75% low melting point agarose dissolved in PBS with EDTA and molded as 48 (7 μL) gels onto GelBond films attached to plastic frames to facilitate subsequent treatment steps. After lysis over night at 4 °C (2.5 M sodium chloride, 0.1 M EDTA, 10 mM Trizma base, 1% lauroylsarcosine sodium salt, pH 10; with 1% Triton X-100 and 10% DMSO freshly added), films were rinsed once and then equilibrated/incubated in enzyme buffer for 50 min prior to enzyme treatment with the bacterial formamidopyrimidine-DNA glycosylase (fpg; 1.0 μg/mL) or left in the same buffer but without the fpg enzyme (1 h, 37 °C). DNA unwinding was performed in electrophoresis buffer in the dark (5 + 35 min, 4 °C). After electrophoresis at 8–10 °C (0.8 V/cm, 20 min, pH 13.2) and neutralization (0.4 M Trizma base buffer pH 7.5 for 2 × 5 min), films were fixed in ethanol and dried. Rehydrated films were stained with SyrbGold (10,000× dilution in Tris–EDTA buffer, pH 8.0, 20 min in the dark) and scored with the Comet IV capture system (version 4.11) from Perceptive Instruments (UK). All samples were blinded and 30 nuclei per gel window were counted. The level of DNA damage was expressed as tail intensity, i.e. % fluorescence in the comet tail relative to the total fluorescence of the comet.

2.8. DNA adduct analysis by ^{32}P-postlabelling

DNA was isolated using a standard phenol/chloroform extraction protocol. For DNA adduct analysis by 1,3-DNP and 1.8-DNP the butanol enrichment procedure of the ^{32}P-postlabelling method was used; B[*a*]P-derived DNA adducts were enriched using nuclease P1 digestion. The procedures were essentially as described previously with minor modification [49,50]. Briefly, DNA (4 μg) was digested with 288 mU micrococcal nuclease (Sigma, UK) and 1.2 mU spleen phosphodiesterase (MP Biomedical, UK), enriched and labeled as reported. Chromatographic conditions for thin-layer chromatography (TLC) on polyethyleneimine-cellulose (Macherey-Nagel, Düren, Germany) were: D1, 1.0 M sodium phosphate, pH 6.0; D3, 4 M lithium formate and 7 M urea, pH 3.5; and D4, 0.8 M lithium chloride, 0.5 M Tris and 8.5 M urea, pH 8.0. After chromatography, TLC sheets were scanned using a Packard Instant Imager (Dowers Grove, IL), and DNA adduct levels (relative adduct labeling [RAL]) were calculated from adduct c.p.m., the specific activity of [γ-^{32}P]ATP and the amount of DNA (pmol of DNA-P) used.

2.9. Gene expression profiling of genes linked to the UPR and inflammation

2.9.1. Microarray analysis

Hepa1c1c7 cells were grown in 90 mm culture dishes (7×10^5 cells/dish) and exposed to the test compounds for 6 h. After incubation and removal of the cell supernatant, cells were stored in RNA later at room temperature until processing. Total RNA was extracted using the RNAqueous Micro Kit (Ambion) according to the manufacturer's instructions. RNA quantity and purity were assessed using a Nanodrop® spectrophotometer. The integrity of the RNA was examined using the Agilent Bioanalyzer 2100 to obtain an RNA integrity number (RIN). All samples used in the subsequent gene expression analysis had a RIN of at least 8.5. The nCounter system (Nanostring Technologies, Seattle, WA) was used to quantify the expression levels of 67 pre-defined genes of interest. Each hybridization reaction contained 100 ng of total RNA in a 5 μL aliquot, reporter and capture probes, six pairs of positive spike-in RNA hybridization controls and six pairs of negative control probes. The hybridization reaction proceeded for 21 h at 65 °C.

2.9.2. Real-time reverse-transcription polymerase chain reaction (RT-PCR)

mRNA was reverse transcribed using Superscript II RT (Invitrogen, Carlsbad, CA) to obtain cDNA for gene expression analysis. Using a 7500 Real-Time PCR Machine (Applied Biosystems, Foster City, CA) with TaqMan Universal PCR MasterMix (Applied Biosystems) the PCR protocol involved: 20 s initiation at 50 °C followed by 10 min at 95 °C; 40 cycles of 15 sec amplification at 95 °C; 1 min at 60 °C. Grp78 (Mm00517690_g1), CHOP (Mm01135937_g1), ATF6 (Mm01295317_m1), spliced XBP1 (Mm03464496_m1), total XBP1 (Mm00457357_m1), Nrf2 (Mm00477784_m1), PGK1 (Mm00435617_m1), RPLP2 (Mm00782638_s1). ΔΔCT was calculated using the SDS software v2.2 as described by the manufacturer (Applied Biosystems; Invitrogen, Life Technologies, Burlington, Ontario, Canada).

2.10. Western blotting immunoassay

Hepa1c1c7 and BEAS-2B cells were grown in 90 mm culture dishes (7×10^5 cells/dish), exposed to test substances for 24 h and then washed with PBS. Cells were then frozen, thawed and lysed in 20 mM Tris buffer, pH 7.5, 150 mM NaCl, 1 mM EDTA, 1 mM EGTA, 1% Triton X-100, 2.5 mM sodium pyrophosphate, 1 mM β-glycerophosphate, 1 mM Na_3VO_4, 1 mM NaF, 10 mg/mL leupeptin, 1 mM PMSF, 10 mg/mL aprotinin and 10 mg/mL pepstatin A. After cell lysis, solutions were sonicated, centrifuged (290×*g*), and the supernatant containing the cellular proteins was collected. Protein concentration was measured by using a Bio-Rad DC protein assay kit. A sample of 12.5 μg protein in each well was subjected to 12% or 15% sodium dodecyl sulfate polyacrylamide gel electrophoresis (SDS-PAGE). Blots

were incubated with primary antibodies overnight according to the manufacturer's recommendations, washed and next incubated with horseradish peroxidase-conjugated secondary anti-rabbit, anti-mouse or anti-goat antibodies (1:5000). The Western blots where developed using the SuperSignal® West Dura Extended Duration Substrate system (Thermo Scientific, Rockford, IL, USA) and a ChemiDox™ XRS+ molecular imager with Image Lab™ software (Bio-Rad Laboratories Inc., Hercules, CA, USA). Typical results are from one out of three separate exposures/experiments.

In experiments linked to UPR, the protein samples were loaded onto 10% SDS-PAGE. Proteins were transferred using a wet transfer apparatus onto a PVDF membrane (Bio-rad) and immunoblotted using antibodies from Santa Cruz Biothecnology against Grp78, Calnexin, and PDI. β-Actin was used in all Western blots as housekeeping protein. Antibodies were diluted in Odyssey Blocking Buffer (1:1000). A two color Western blot infrared fluorescent detection method was used to visualize the proteins using IRDye fluorescent secondary antibodies and Odyssey® Imager (LI-COR Biosciences). Quantification of fluorescent Western blot was achieved with ImageJ program designed by the NIH.

2.11. Statistical analysis

For the statistical analysis of Nanostring data, the nSolver Analysis Software v1.1 (Nanostring Technologies) was used to normalize the raw gene expression data to the positive controls and 12 reference genes: *ACTB*, *B2 M*, *GAPDH*, *GUSB*, *HPRT1*, *IPO8*, *PGK1*, *POLR2A*, *RPLP2*, *TBP*, *UBC* and *YWHAZ*. One-way ANOVA analysis was conducted using GraphPad Prism 5.0 (GraphPad Software, Inc, San Diego, CA, USA). Unsupervised hierarchical clustering was performed with Multiexperiment Viewer 4.9 using Euclidian distance with average linkage clustering. The other results were representatives of three or more independent experiments with identical conditions. Data was presented as mean ± SEM. Statistical significance was evaluated using analysis of variance (ANOVA) with the Dunnet post-test. To analyze the effect of treatment on cytotoxicity, ROS, comet assay and RT-PCR responses statistics was performed on log-transformed data. $P < 0.05$ was considered significant. All calculations were executed with GraphPad Prism software.

3. Results

3.1. Cell death

BEAS-2B cells and Hepa1c1c7 cells were treated with 1,3-DNP and 1,8-DNP for 24 and 72 h, or DMSO only as control. Toxicity was examined by light microscopy (data not shown) and quantified after the staining of cells with Hoechst 33342 and PI. No major cytotoxic effects were observed in BEAS-2B cells after exposure to 1,3-DNP and 1,8-DNP (Fig. 2). In Hepa1c1c7 cells (Fig. 2), however, 1,3-DNP caused a concentration-dependent increase in cell death starting at 3 μM after 24 h exposure. The induced cell death was a mixture of apoptosis and necrosis. In contrast, 1,8-DNP did not induce any significant cell death after 24 h; after 72 h increased cell death was observed at the highest concentration (30 μM; Fig. 2).

3.2. Characterization of apoptosis

We further characterized the 1,3- and 1,8-DNP-induced cell death in Hepa1c1c7 cells. After exposure to various concentrations of DNPs for 24 h, Hepa1c1c7 cells were sampled and analyzed by Western blotting. This revealed an increased cleavage of pro-caspase 3 and PARP at 10 and 30 μM 1,3-DNP (Fig. 3A), while 1,8-DNP had no effects. Further, the pan-caspase inhibitor zVAD-FMK reduced 1,3-DNP-induced apoptosis from 31% to less than 15% (Fig. 3B), but the necrosis was somewhat increased.

Effects on cell cycle were analyzed by flow cytometry after 24 h of exposure (Fig. 3C). 1,3- and 1,8-DNP (10 μM) both decreased the number of cells in G1, and increased the number of cells in S phase. 1,3-DNP seemed to be slightly more potent than 1,8-DNP, and also gave a significant G2 increase even at 3 μM.

3.3. Cellular mechanisms involved in the cytotoxicity

ROS may be formed during nitro-PAHs metabolism as well as during the cell death process as a result of mitochondrial damage. As it has been suggested that ROS is an important determinant both with regard to induced cytotoxicity and genotoxicity, we measured ROS formation in BEAS-2B and Hepa1c1c7 cells after exposure to various concentrations of 1,3- and 1,8-DNP for 2 and 24 h (Fig. 4; Supplementary Fig. 1). Both compounds increased the level of ROS as determined by CM-H_2DCFDA-fluorescence detecting hydrogen peroxide. In BEAS-2B cells, both compounds showed significant responses after both 2 and 24 h exposure, with 1,8-DNP giving a slightly larger response. In Hepa1c1c7 cells, 1,8-DNP was the only compound that increased ROS after 2 h; and clearly giving a more robust response than 1,3-DNP. ROS formation/mitochondria function can also be determined by DHE-fluorescence measuring superoxide anions. As shown in Fig. 5 and Supplementary Fig. 2, the only positive response was seen at 10 μM 1,8-DNP in BEAS-2B cells.

3.4. DNA damage

To examine if the cytotoxic response observed by 1,3-DNP in Hepa1c1c7 cells is due to DNA damage and/or to test if the increased ROS resulted in oxidative damage to DNA, the comet assay was used. The alkaline comet assay measures SSBs and alkali-labile sites, however, the use of the fpg-modified comet assay also allows the detection of oxidized bases such as 7,8-dihydro-8-oxoguanine (8-oxoG) and various ring-opened purines [48,51]. In BEAS-2B cells both DNPs showed no response in the comet assay without fpg (Fig. 6A), while the assay was positive in Hepa1c1c7 cells with 1,8-DNP being slightly more potent (Fig. 6B). In BEAS-2B cells both 1,3-DNP and 1,8-DNP increased the level of oxidative damage to DNA at 3 μM, while a marked response in Hepa1c1c7 cells was first seen at somewhat

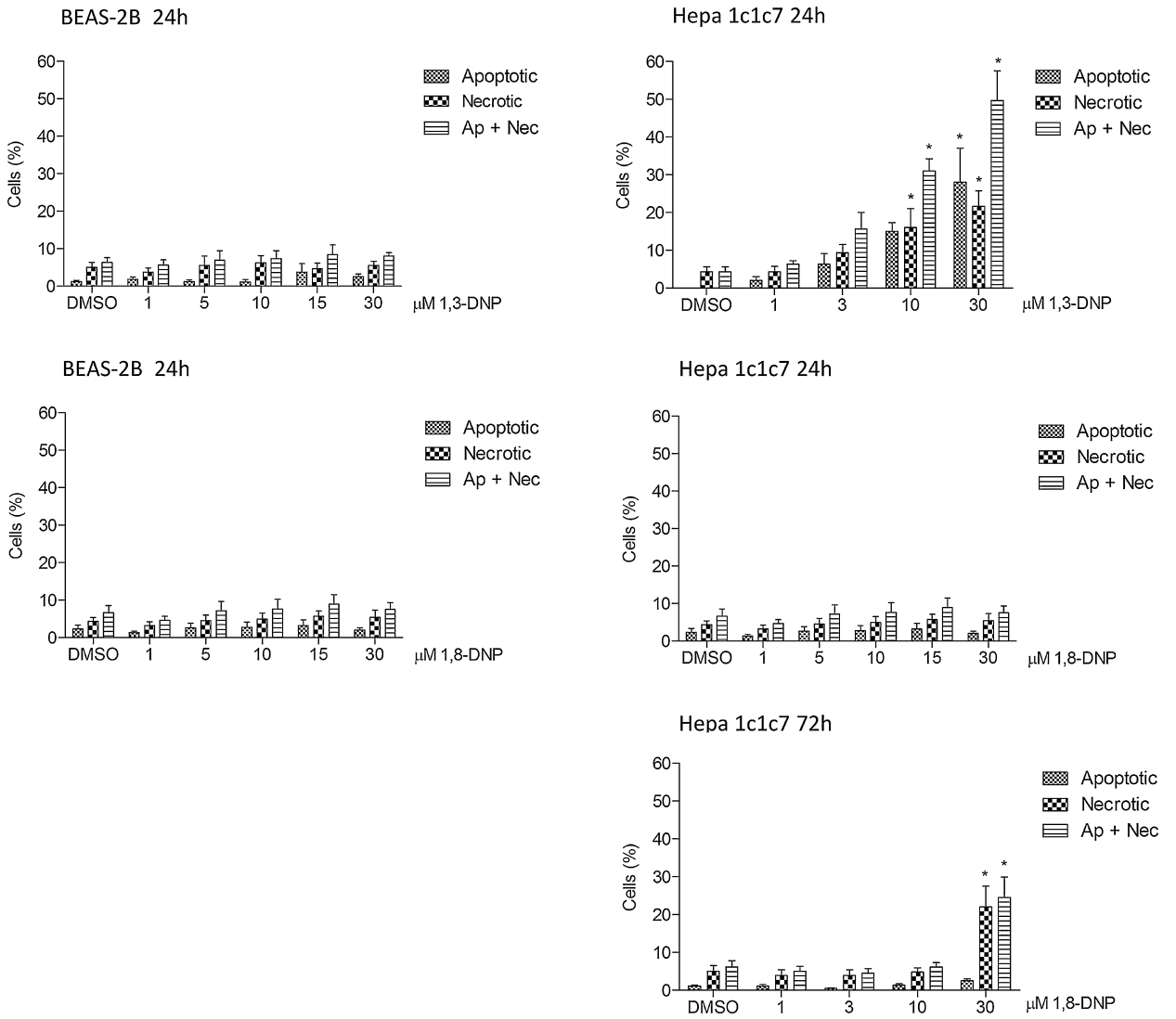

Fig. 2. Cell death determined by fluorescence microscopy. BEAS-2B or Hepa1c1c7 cells were exposed to various concentrations of 1,3-DNP, 1,8-DNP or DMSO (control) for up to 72 h. Cells were stained with Hoechst 33342 and propidium iodide (PI), and subsequently analyzed for apoptosis (Ap) (including apoptotic necrotic) and necrosis (Nec) using fluorescence microscopy. The third columns in the graphs are the sums of the two first. Data presents the mean ± SEM of at least 3 independent experiments. * Significantly different from DMSO-treated controls ($p < 0.05$).

higher concentrations (Fig. 6A and B). These results corresponded roughly to measured ROS production (see above). Furthermore, we found that in BEAS-2B cells only 1,8-DNP resulted in DNA adduct formation as measured by the ^{32}P-postlabelling assay (Fig. 6C and D). Adduct levels were lower than those reported in a previous study using Hepa1c1c7 cells. In that study also1,8-DNP but not 1,3-DNP induced DNA adducts [14].

3.5. DNA damage response

To investigate if the differences in toxicity between these two strongly related DNPs could be explained by differences in their DDR, we looked at the phosphorylation of H2AX and p53 by Western blotting. H2AX is phosphorylated at serine 139 (γH2AX) upon induction of DSB. It is often used as an indicator of DSB formation [52] which is considered to be a particular lethal DNA damage. In BEAS-2B cells DNP treatment only lead to a slight increase in the γH2AX formation (Fig. 7A); while marked responses were obtained in Hepa1c1c7 cells after exposure to low concentrations of both DNPs. 1,8-DNP induced stronger γH2AX responses compared to 1,3-DNP, and 1,8-DNP also seemed to induce these effects at lower concentrations (Fig. 7B). Similarly, little effects in BEAS-2B and a stronger effect of DNPs in Hepa1c1c7 cells were seen with regards to p53 phosphorylation, an important transcription factor particularly for genes controlling cell cycle arrest and/or apoptosis [37,53–56]. After exposure the Hepa1c1c7 cells to 1,8-DNP, a marked concentration-dependent increase in phosphorylated p53 was already seen at 1 μM. In contrast, only slight increases were observed after 1,3-DNP exposure at higher concentrations (Fig. 7).

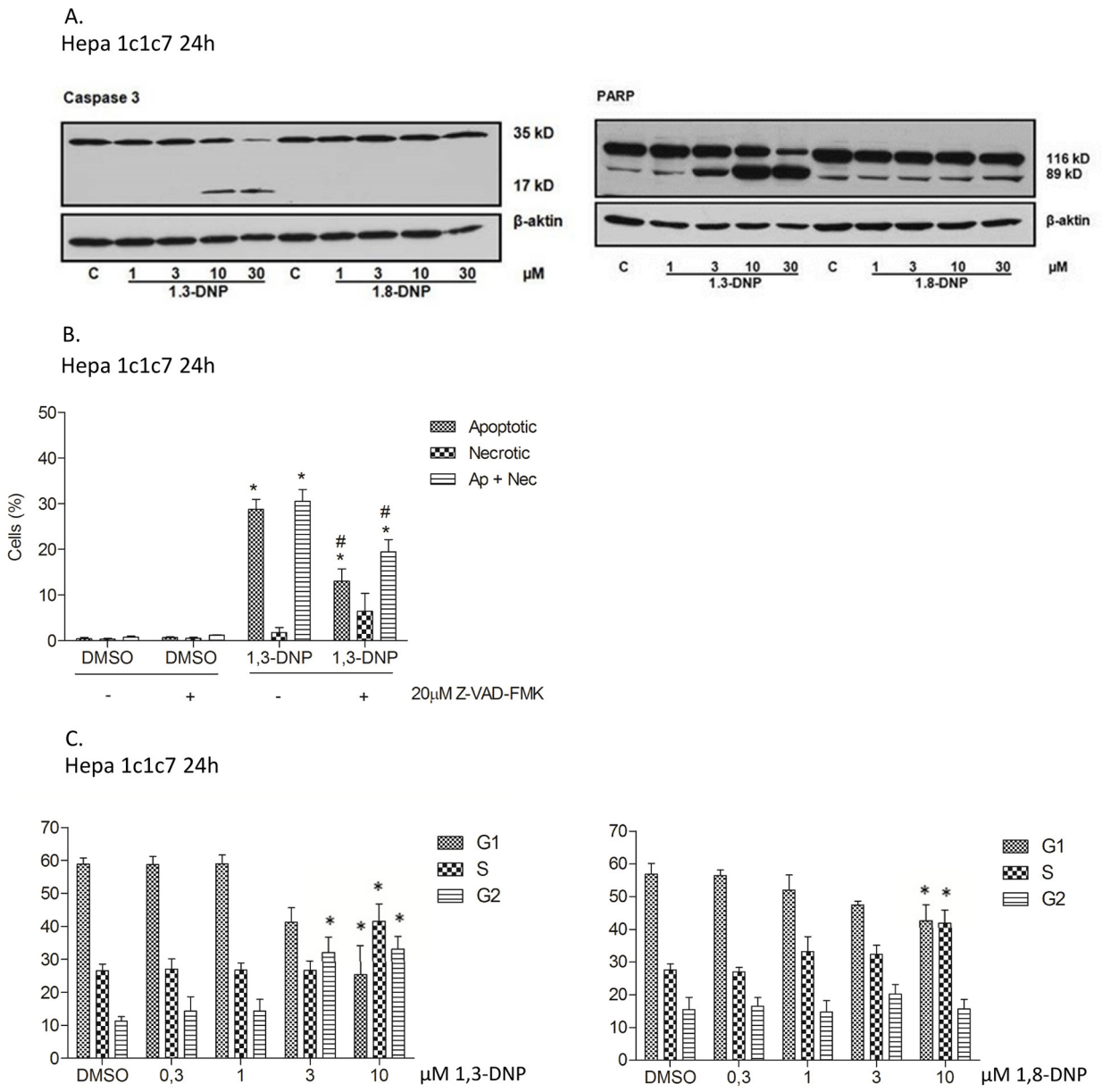

Fig. 3. Effects of 1,3-DNP and 1,8-DNP apoptosis on cell cycle distribution. Hepa1c1c7 cells were exposed to various concentrations of 1,3-DNP, 1,8-DNP, or DMSO (control) for 24 h. (A) Levels of PARP and caspase 3 were analyzed by Western blotting (shown is one representative experiment out of three separate incubations). (B) Hepa1c1c7 cells were pre-treated for 1 h with zVAD-FMK (20 μM) followed by co-exposure with 1,3-DNP (30 μM) or DMSO (control) for 24 h. Percentage of cell death was estimated by fluorescence microscopy counts. Data presents the mean ± SEM of 3 independent experiments. * Significantly different from DMSO-treated controls ($p < 0.05$). # Significantly different from treatments without zVAD-FMK ($p < 0.05$). (C) Hepa1c1c7 cells were exposed to various concentrations of 1,3-DNP, 1,8-DNP or DMSO (control) for 24 h. Cells were stained with Hoechst 33258 and the cell cycle distribution was measured by flow cytometer. Data is presented as the relative proportions of cells (%) in the different cell cycle phases. Each bar represents the mean ± SEM of 3 independent experiments. *Significantly different from DMSO-treated controls ($p < 0.05$).

Pifithrin-α (PFT-α) suppresses p53-mediated transcription, while pifithrin-μ (PFT-μ) inhibits p53 located to the mitochondria by reducing its affinity to the anti-apoptotic proteins Bcl-xl and Bcl-2 [57]. Fluorescence microscopy analyses after Hoechst 33342 and PI staining showed that PFT-α almost completely inhibited 1,3-DNP-induced cell death (Fig. 8A), while PFT-μ was clearly less effective suggesting that p53-mediated transcription is required for this apoptotic process.

3.6. Effects on ER-stress and UPR

Although 1,8-DNP induced considerably more ROS and DNA damage as well as stronger DNA-DR and p53

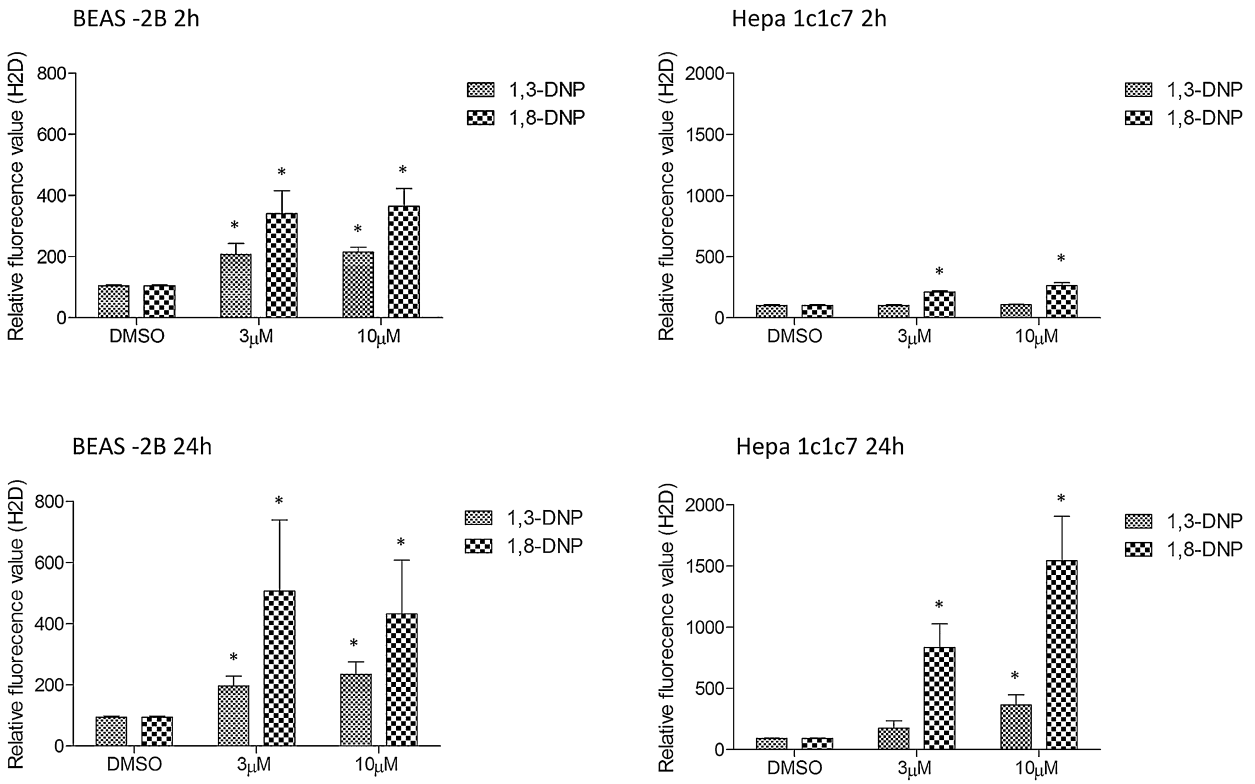

Fig. 4. ROS as determined by H2DCFDA-fluorescence. BEAS-2B or Hepa1c1c7 cells were exposed to various concentrations of 1,3-DNP, 1,8-DNP, or DMSO (control) for 2 or 24 h. During the last 2 h CM-H2DCFDA (H2D in figure) was added. After exposure cells were analyzed by flow cytometer (see also Supplementary Fig. 1). Each bar represents the mean ± SEM of 3 independent experiments. *Significantly different from DMSO-treated controls ($p < 0.05$).

activation, 1,8-DNP induced little apoptosis compared to 1,3-DNP. Thus, additional pathways are likely involved in the apoptotic process induced by 1,3-DNP. One of such pathways could be ER stress and subsequent UPR, which has recently been found to be triggered by various environmental factors [27]. In order to explore this possibility we exposed the cells to the DNPs for 6 h and examined their effect on gene expression linked to UPR. First, we used Nanostring's nCounter technology to analyze RNA expression profiling for 67 primary genes linked to UPR and inflammation. As shown in Fig. 9A and B, 1,3-DNP but not 1,8-DNP induced a increase in *AFT4*, *Grp78* and *XBP1* gene expression, all of which are linked to the UPR response. In line with a stronger UPR also the increase of *AFT6*, *CHOP* was marked higher for 1,3-DNP than 1,8-DNP. Interestingly, 1,3-DNP also increased the MAPK-related gene *TAOK3*, and genes linked to inflammation (e.g. *IL-6*). However, no release of IL-6 was seen in BEAS-2B or Hepa1c1c7 cells (data not shown). Unsupervised hierarchical clustering was used to identify subgroups of genes and samples with similar expression patterns. The nine samples in our dataset were successfully grouped into their respective treatment groups based solely on their gene expression profiles. 1,3-DNP-treated cells were identified as a distinct cluster from the control and the 1,8-DNP-treated cells. The aforementioned UPR genes and inflammatory markers were also sorted into a unique gene cluster. The cluster was characterized by increased expression of its component genes in the 1,3-DNP samples compared to the controls. A similar trend of 1,3-DNP-induced UPR activation was verified in independent experiments using RT-PCR (data not shown).

4. Discussion

1,3-DNP and 1,8-DNP are both reported to be genotoxic and induce tumors in rats, but 1,8-DNP is considered to be the most potent [6,41,42]. In previous studies we have found that human lung epithelial BEAS-2B cells are more sensitive to 3-nitrobenzanthrone (3-NBA)-induced DNA damage and cell death than Hepa1c1c7 cells, while B[*a*]P and 1-nitropyrene (1-NP) appear to be more toxic in Hepa1c1c7 cells [35,37,58]. In the present study we found that BEAS-2B cells were less responsive than Hepa1c1c7 cells to 1,3- and 1,8-DNP with regards to cytotoxicity, DNA adduct formation and DDR. However, the two DNPs induced at least as much ROS and even more oxidative damage to DNA in BEAS-2B cells than in Hepa1c1c7 cells. It is noteworthy that 1,3-DNP induced an apoptosis in Hepa1c1c7 cells which was depending on p53 transcriptional activity. In contrast, 1,8-DNP induced no apoptosis despite more DNA adducts, a larger DDR and a considerably stronger p53 activation implying a role of additional mechanism(s) for the resulting apoptosis. In line with this, we observed that 1,3-DNP but not 1,8-DNP, induced activation of several UPR-response genes, including the apoptosis-related *ATF4* gene and it

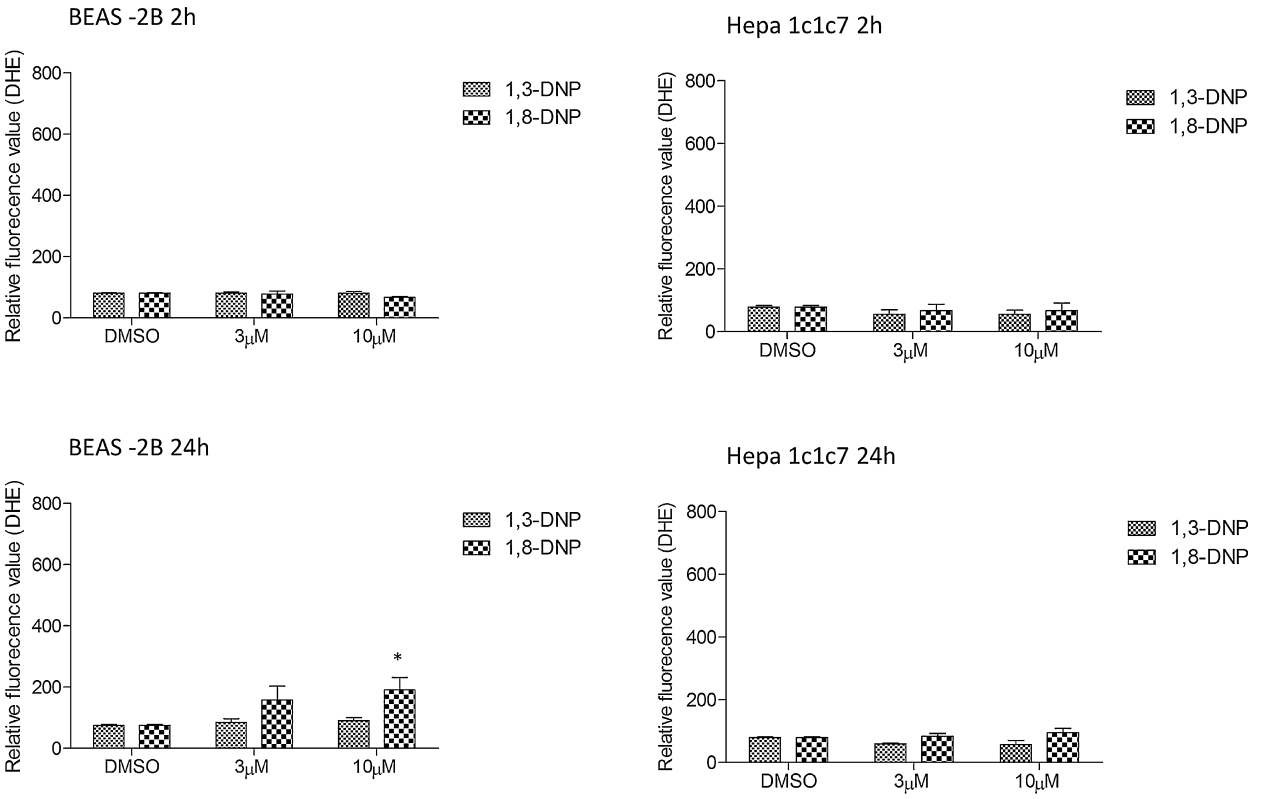

Fig. 5. ROS as determined by DHE-fluorescence. BEAS-2B or Hepa1c1c7 cells were exposed to various concentrations of 1,3-DNP or 1,8-DNP, or DMSO (control) for 2 or 24 h. During the last 2 h DHE was added. After exposure cells were analyzed by flow cytometer (see also Supplementary Fig. 2). Each bar represents the mean ± SEM of 3 independent experiments. *Significantly different from DMSO-treated controls ($p < 0.05$).

downstream mediator *CHOP*. Thus, we suggest that the stronger mutagenic/carcinogenic potency of 1,8-DNP compared to 1,3-DNP is linked to its greater DNA damage properties, which in combination with its lower potency to induce cell death increases the probability of inducing mutations.

Both DNPs induced cell death to various extents in the two different cell lines. In BEAS-2B cells neither 1,3-DNP nor 1,8-DNP exposure resulted in increased cell death. We have previously shown that exposure of diesel exhaust particles result in an increased release of cytokines in BEAS-2B, and related this response to chemical pollutants bound to the particles [40,59]. One major chemical compound linked to urban air PM was 1-NP, which increased production of the cytokines IL-6 and IL-8 in BEAS-2B cells [37]. ROS has often been regarded to be an important triggering factor for increased cytokine production/release by ambient air particles as well as organic pollutants attached to them [40]. However, in the present study we did not observe any effect on the release of IL-6 and IL-8 after 1,3-DNP or 1,8-DNP exposure (data not shown). Interestingly, this was despite the fact that both compounds markedly induced ROS and oxidative damage to DNA in BEAS-2B cells, without an increase in cytotoxicity. This observation is in line with previous findings from our group suggesting that oxidative stress alone is insufficient for cytokine responses in the BEAS-2B cell line [37,60]. This implies that while ROS may be an important determinant for activation of cytokine responses, additional signals are required.

In BEAS-2B cells 1,3-DNP and 1,8-DNP rapidly enhanced ROS formation to a level which was sustained for 24 h after exposure, suggesting the rate of ROS formation for both DNPs was long-lasting. Increased ROS levels were found to be accompanied by a marked increase in oxidative damage to DNA as measured by the comet assay. However, little, if any, increase in SSB-levels was observed (comet assay without fpg), indicating that the oxidative damage to DNA may have been repaired in a balanced way in these cells. Further studies e.g. with DNA repair inhibitors are needed to assess the actual rate of formation of the oxidative damage to DNA and damage removal in these cells.

We have previously shown that winter urban air $PM_{2.5}$ from Milan containing a high level of PAH, could cause mitotic delay, mitotic catastrophe and/or apoptosis in BEAS-2B cells [36]. So far tested neither various diesel exhaust PMs, B[*a*]P, 1-NP, 3-NBA nor various quinones have been found to induce such effects in BEAS-2B [35,40,61]. However, 3-NBA which is activated by the nitroreductase NAD(P)H:quinone oxidoreductase (NQO1) was found to be a potent inducer of DNA adducts and apoptosis [35]. In the present study we found that although both DNPs induced ROS and oxidative damage to DNA, little DDR, no cell death and no marked effects on proliferation (visual examination; data not shown) were observed in the

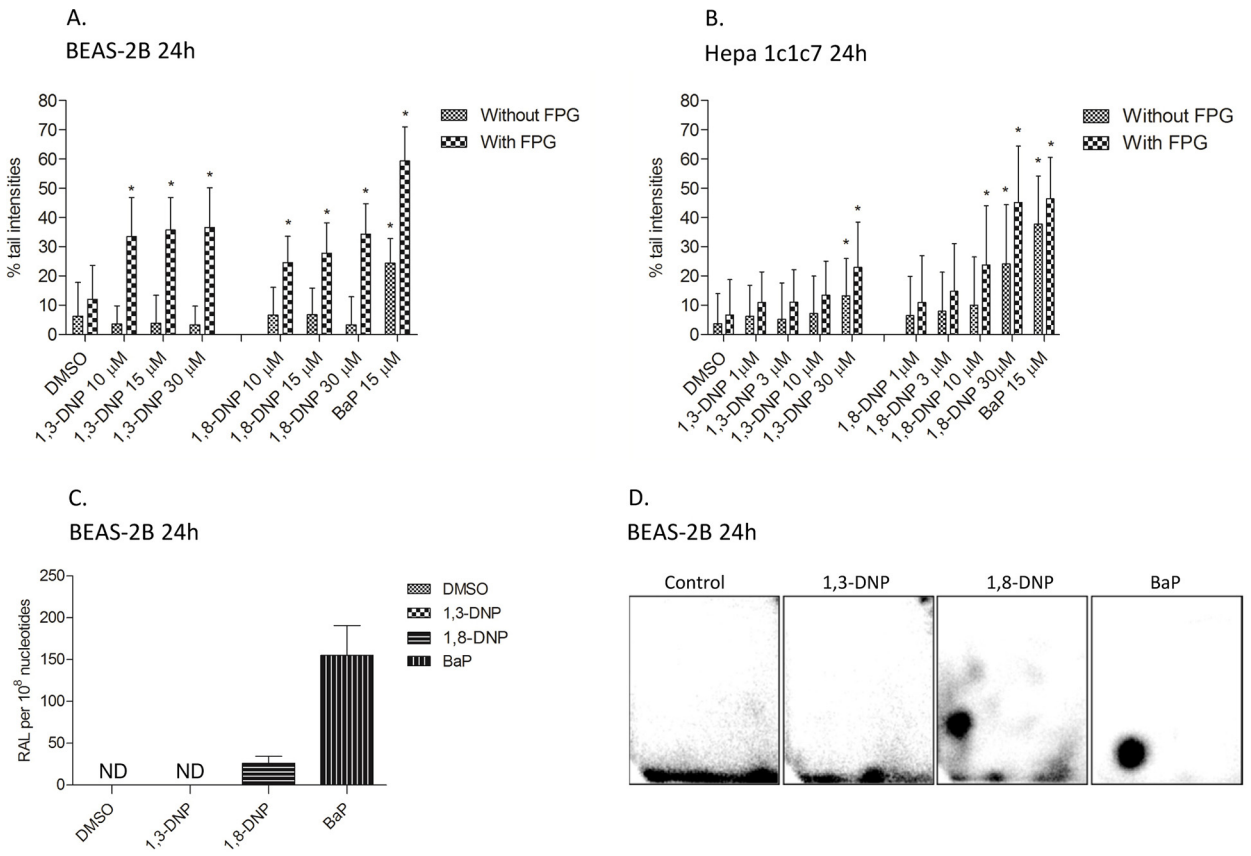

Fig. 6. DNA damage measured by the comet assay and DNA adduct formation assessed by ^{32}P-postlabelling. BEAS-2B (A, C) and Hepa1c1c7 (B) cells were exposed to 1, 3, 10 or 30 μM of 1,3-DNP, 1,8-DNP, B[*a*]P (15 μM) or DMSO (control) for 24 h. DNA strand breaks were measured by the comet assay (without fpg), and oxidative damage to DNA was determined using the fpg-modified comet assay (A and B). Data (% tail DNA) represents the mean ± SEM of 3 independent experiments. (C and D) DNA adduct formation (RAL, relative adduct labeling) in BEAS-2B was measured by ^{32}P-postlabelling assay. ND, not detectable.

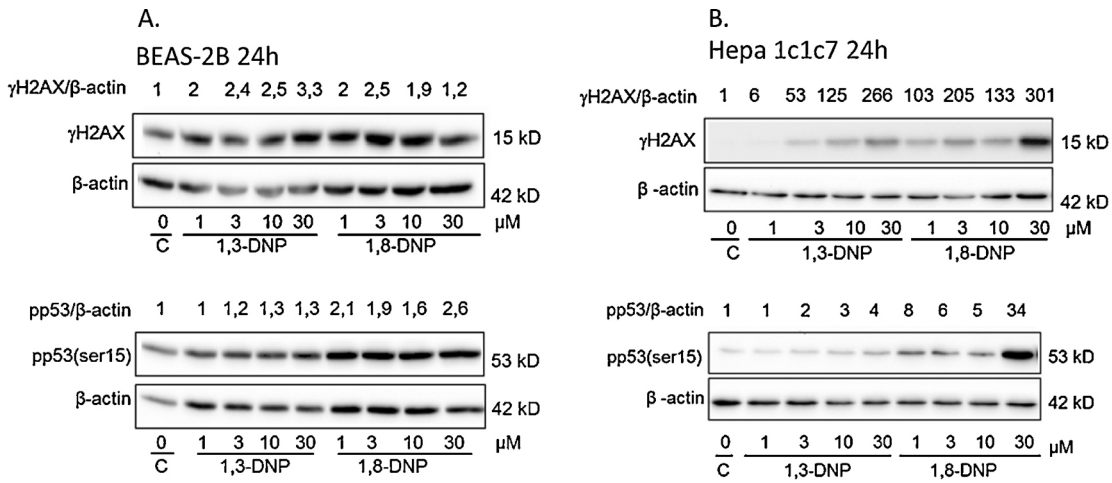

Fig. 7. The effect on DNA damage response. BEAS-2B (A) and Hepa1c1c7 cells (B) were exposed to various concentrations of 1,3-DNP, 1,8-DNP or DMSO for 24 h and levels of H2AX, phosphorylated H2AX (γH2AX) and p53 were analyzed by Western blotting (semi quantification are given as numbers above the blots). Results from one representative of three separate experiments are presented.

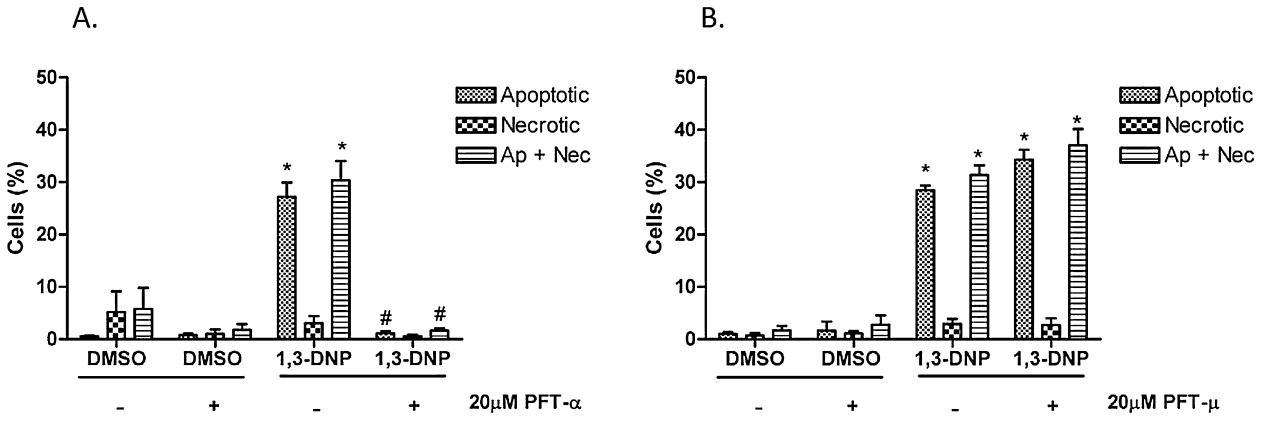

Fig. 8. Effects of p53 inhibitors on 1,3-DNP induced cell death. Hepa1c1c7 cells were exposed to 10 μM 1,3-DNP for 24 h with or without pre-incubation for 1 h with 20 μM pifithrin-α (PFT-α, A) or PFT-μ (B). Control cells were treated with DMSO only. Cells were stained with Hoechst 33342 and propidium iodide (PI), and subsequently analyzed for apoptosis (Ap) (including apoptotic necrotic) and necrosis (Nec) using fluorescence microscopy. *Significantly different from DMSO-treated controls. #Significantly different from treatment without inhibitor ($p < 0.05$).

BEAS-2B cells. Thus, apparently some other/stronger signals are needed to induce these effects. The lack of response in BEAS-2B cells when compared to Hepa1c1c7 cells may be linked to their lower CYP enzyme levels resulting in lower PAH metabolism [62,63]. The high ROS responses observed suggest that nitro-reduction reactions resulting in ROS dominate in BEAS-2B cells. Furthermore, the lower amount of 1,8-DNP-DNA adducts formed in BEAS-2B relative to Hepa1c1c7 cells [14] may suggest metabolic differences not only with regards to the expression of CYP enzymes. These metabolic differences could have impact on DNA adduct formation.

While both DNPs were not cytotoxic in BEAS-2B cells, 1,3-DNP induced a concentration-dependent increase in cell death in Hepa1c1c7 cells after 24 h, starting at concentrations of ≥3 μM. In contrast, 1,8-DNP only induced cell death after prolonged exposure at much higher concentrations (30 μM at 72 h). In previous studies we have found that various PAHs and nitro-PAHs have resulted in different forms of cell death. For example, exposure to B[*a*]P was linked to a mixture of apoptosis and necrosis, 1-NP to apoptosis and a non-apoptotic programmed cell death [13], and 3-nitrofluoranthrene to apoptosis and a programmed cell death with necroptotic features [34]. Judged by microscopic examination and Western blot analysis, the 1,3-DNP-induced cell death was a mixture of apoptosis and necrosis. Similar results were previously reported for B[*a*]P [64]. Because the pan-caspase inhibitor zVAD-FMK only partially inhibited 1,3-DNP-induced cell death, we cannot exclude that there is an alternative caspase-independent pathway as reported previously for 1-NP [65]. This mixed picture which is often seen after chemical exposure is probably due to an incomplete apoptotic process in many of the cells due to the apoptotic process being switched to necrosis, possibly as a result of mitochondrial damage and low ATP levels, and/or inactivation of caspases as suggested previously [64,66,67].

Differences in DNA adduct formation after 1,3- and 1,8-DNP exposure may be due to differences in metabolism [68]. The activation/detoxification pathways for both nitro-PAHs are not precisely known. Differences in their nitro-reduction have been reported. While 1,3-DNP is reduced by a nitroreductase transferring a single electron, 1,8-DNP is reduced by an enzyme that transferring two electrons [69]. However, no clear relationship has been found for 1,8-DNP between DNA adduct formation and NQO1 expression in a panel of mouse embryonic fibroblast cell lines [49]. Other nitroreductases such as xanthine oxidase have also been shown to activate nitro-PAHs like 3-NBA [1,70]. Inactivation of 1,3- and 1,8-DNPs by human liver microsomal P450s has been reported [9]. Other studies indicate that 1,6-DNP, and 1,8-DNP can be activated by human P450 1B1 [68]. Collectively, these findings suggest that mechanisms involved in the activation and detoxification of NP is complex and may depend on the chemical as well as the experimental system used.

In this study we observed that 1,8-DNP induced more DNA damage, a stronger DNA-DR response, and a stronger activation of p53 than 1,3-DNP. Nevertheless, p53 inhibition with pifithin-α (PFT-α) markedly reduced cell death induced by 1,3-DNP in the Hepa1c1c7 cells, while PFT-μ had no effect. This suggests that transcriptional activity of p53 is required to execute the 1,3-DNP-induced apoptotic process. In line with this finding we have previously observed that B[*a*]P-induced DNA damage was associated with a p53-dependent cell death in these cells [64]. It is noteworthy that in a previous study we observed that 1,8-DNP induced p53 phosphorylation in Hepa1c1c7 cell, but this was not accompanied by nuclear translocation [14]. Therefore, we suggested that the inability of phosphorylated p53 to enter the nucleus in 1,8-DNP-exposed Hepa1c1c7 cells, could explain the lack of cell death. However, in the present study, p53 did appear to translocate to the nucleus following 1,8-DNP exposure in Hepa1c1c7 cells (data not shown). It remains to be clarified whether this discrepancy may be related to batch/passage differences of the Hepa1c1c7 cells. Nevertheless, 1,8-DNP failed to induce apoptosis in the present study, despite the apparently functional p53-translocation. Thus it is possible that the 1,8-DNP-induced p53-activation alone is insufficient to trigger apoptosis, and that additional p53-independent cellular signals are needed for a cytotoxic response.

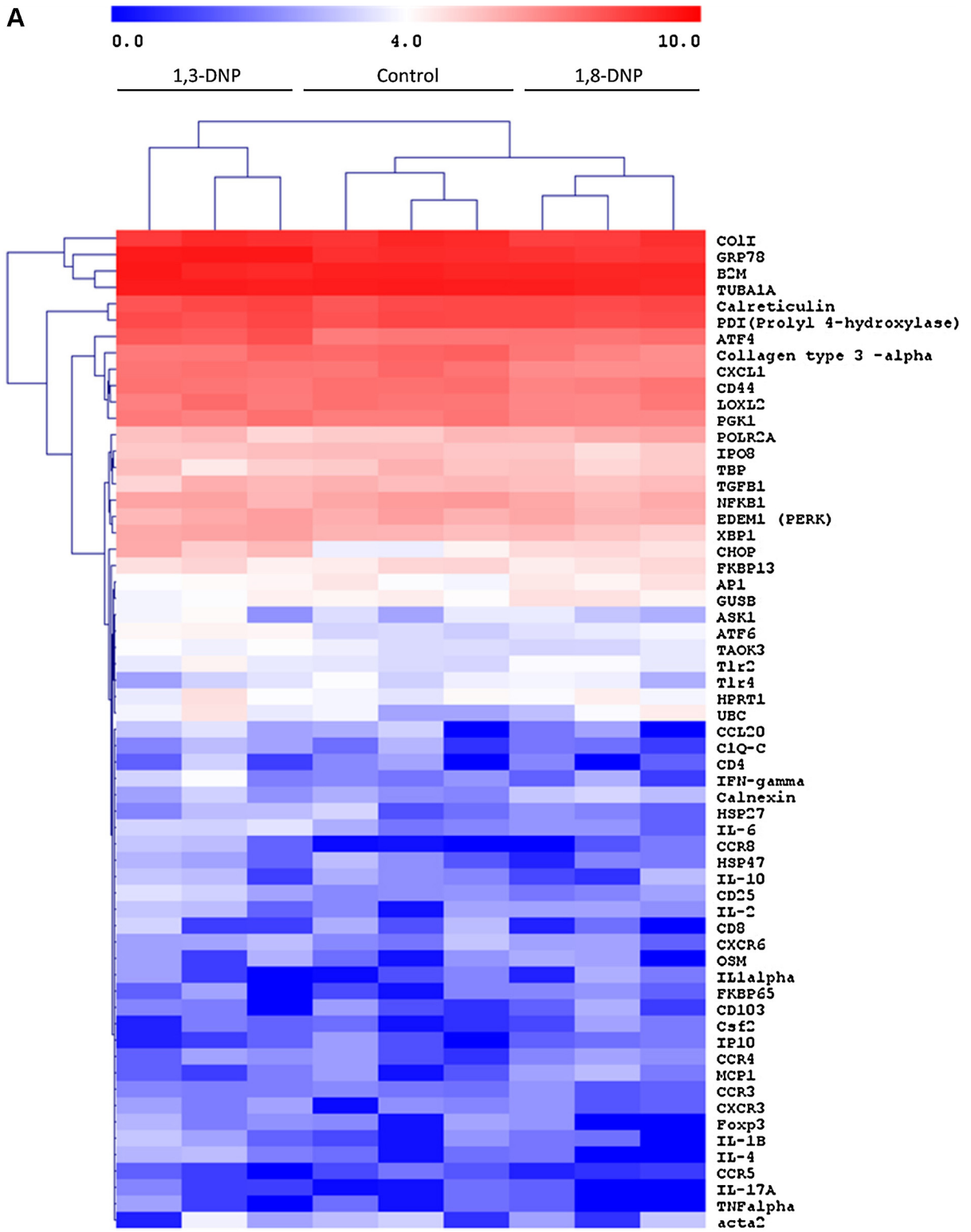

Fig. 9. Effects on protein unfolding response (UPR). Hepa1c1c7 cells were exposed to 10 μM 1,3-DNP or 1,8-DNP for 6 h and gene expression was measured by NanoString's nCounter technology. A heat map showing fold changes for the 1,3-DNP and 1,8-DNP cells (A). Each column represents an individual cell culture sample. Changes in gene expression were calculated using the $\log_2$-transformed fold ratios between each experimental sample and the mean of the controls. Hierarchical clustering was performed using Euclidian distance and average linkage. A histogram demonstrating the $\log_2$-fold ratios for selected UPR genes and IL-6 (B). Each bar represents the mean fold change ± SEM of three replicates for each treatment condition. $^{*}p < 0.05$, $^{**}p < 0.01$, $^{***}p < 0.001$ vs. DMSO-treated controls.

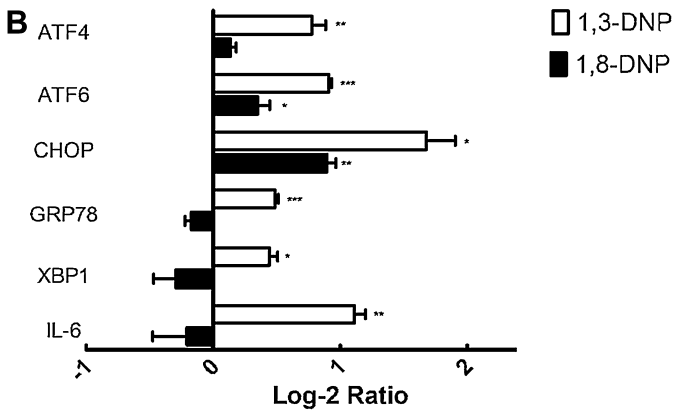

Fig. 9. (*Continued*)

In contrast to 1,8-DNP, 1,3-DNP induced ER-stress and UPR as judged by increased expression of several UPR response genes. Of particular interest is that 1,3-DNP induced increased expression of *ATF4* and its downstream target *CHOP*, which are both considered to be among the main effectors of UPR-induced apoptosis (30). Recent findings showed that over-expression of *ATF4* and *CHOP* induced apoptosis, through increased protein synthesis, ATP depletion and ROS-formation [71]. This suggests that the increase in *ATF4* and *CHOP* expression may have contributed to 1,3-DNP-induced apoptosis in the present study, and that ER-stress and UPR plays a central role in the induced cell death. Thus, despite inducing only moderate DNA damage and DDR, 1,3-DNP appears to induce more cytosolic damage than 1,8-DNP thereby triggering additional death signals. This suggests that cross-talk between DDR and cytotoxic signaling from the cytosol may be central in determining whether DNA damage results in cell cycle arrest and DNA repair, or triggers apoptosis in 1,3-DNP exposed Hepa1c1c7 cells. In concordance with this, reactive metabolites known to preferentially react with DNA compared to other macro-molecules are known to have a higher mutagenic potential [72]. Further studies are needed to explore these hypotheses, which may be very important when evaluating various chemicals for their carcinogenic properties.

5. Conclusion

This study showed that a small change in molecular structure, such as changing the position of a nitro group from 3rd position to 8th position can have marked impact on the cellular response. The observed effects were markedly different depending on the cellular model used. BEAS-2B cells responded with more ROS and oxidative damage to DNA, while Hepa1c1c7 cells seemed to be a more sensitive cellular model with regards to DNA adduct formation, DDR (1,8-DNP), and cell death (1,3-DNP). Our results indicate that both DDR and UPR play central roles in 1,3-DNP-induced apoptosis in Hepa1c1c7 cells. Our data suggests that the stronger carcinogenic potency of 1,8-DNP compared to 1,3-DNP is linked to its higher genotoxic effects, which in combination with its lower potency to induce cell death may increase the probability of causing mutations.

Conflict of interest statement

The authors declare no conflicts of interest.

Acknowledgements

We thank Hans-Jørgen Dahlman for assistance with the flow cytometer. The work was supported by the Research Council of Norway, through the Environment, Genetics and Health-program (grants no. 165386 and 160863). Volker M. Arlt is supported by Cancer Research UK. Kjetil Ask is supported by the Canadian Lung Association and Ontario Thoracic Society.

Appendix A. Supplementary data

Supplementary material related to this article can be found, in the online version, at doi:10.1016/j.toxrep.2014.07.009.

Transparency document

The Transparency document associated with this article can be found in the online version.

References

[1] V.M. Arlt, 3-Nitrobenzanthrone, a potential human cancer hazard in diesel exhaust and urban air pollution: a review of the evidence, Mutagenesis 20 (2005) 399–410.
[2] E. Garshick, F. Laden, J.E. Hart, B. Rosner, T.J. Smith, D.W. Dockery, F.E. Speizer, Lung cancer in railroad workers exposed to diesel exhaust, Environ. Health Perspect. 112 (2004) 1539–1543.
[3] M.C. Turner, D. Krewski, C.A. Pope, 3rd, Y. Chen, S.M. Gapstur, M.J. Thun, Long-term ambient fine particulate matter air pollution and lung cancer in a large cohort of never-smokers, Am. J. Respir. Crit. Care Med. 184 (2011) 1374–1381.
[4] A. Nemmar, J.A. Holme, I. Rosas, P.E. Schwarze, E. Alfaro-Moreno, Recent advances in particulate matter and nanoparticle toxicology: a review of the in vivo and in vitro studies, Biomed. Res. Int. 2013 (2013) 279371.
[5] IARC, IARC monographs on the evaluation of carcinogenic risks to humans Diesel and Gasoline Engine Exhausts and Some Nitroarenes, vol. 46, International Agency for Research on Cancer, 1989, pp. 1–458.

[6] S. Takayama, M. Tanaka, Y. Katoh, M. Terada, T. Sugimura, Mutagenicity of nitropyrenes in Chinese hamster V79 cells, Gann 74 (1983) 338–341.
[7] V. Purohit, A.K. Basu, Mutagenicity of nitroaromatic compounds, Chem. Res. Toxicol. 13 (2000) 673–692.
[8] K. El-Bayoumy, A.K. Sharma, J.M. Lin, J. Krzeminski, T. Boyiri, L.C. King, G. Lambert, W. Padgett, S. Nesnow, S. Amin, Identification of 5-(deoxyguanosin-N2-yl)-1,2-dihydroxy-1,2-dihydro-6-aminochrysene as the major DNA lesion in the mammary gland of rats treated with the environmental pollutant 6-nitrochrysene, Chem. Res. Toxicol. 17 (2004) 1591–1599.
[9] T. Shimada, Y. Fujii-Kuriyama, Metabolic activation of polycyclic aromatic hydrocarbons to carcinogens by cytochromes P450 1A1 and 1B1, Cancer Sci. 95 (2004) 1–6.
[10] K. Ask, N. Decologne, N. Asare, J.A. Holme, Y. Artur, H. Pelczar, P. Camus, Distribution of nitroreductive activity toward nilutamide in rat, Toxicol. Appl. Pharmacol. 201 (2004) 1–9.
[11] K. Ask, S. Dijols, C. Giroud, L. Casse, Y.M. Frapart, M.A. Sari, K.S. Kim, D.J. Stuehr, D. Mansuy, P. Camus, J.L. Boucher, Reduction of nilutamide by NO synthases: implications for the adverse effects of this nitroaromatic antiandrogen drug, Chem. Res. Toxicol. 16 (2003) 1547–1554.
[12] N. Asare, M. Lag, D. Lagadic-Gossmann, M. Rissel, P. Schwarze, J.A. Holme, 3-Nitrofluoranthene (3-NF) but not 3-aminofluoranthene (3-AF) elicits apoptosis as well as programmed necrosis in Hepa1c1c7 cells, Toxicology 255 (2009) 140–150.
[13] N. Asare, N.E. Landvik, D. Lagadic-Gossmann, M. Rissel, X. Tekpli, K. Ask, M. Lag, J.A. Holme, 1-Nitropyrene (1-NP) induces apoptosis and apparently a non-apoptotic programmed cell death (paraptosis) in Hepa1c1c7 cells, Toxicol. Appl. Pharmacol. 230 (2008) 175–186.
[14] N.E. Landvik, M. Gorria, V.M. Arlt, N. Asare, A. Solhaug, D. Lagadic-Gossmann, J.A. Holme, Effects of nitrated-polycyclic aromatic hydrocarbons and diesel exhaust particle extracts on cell signalling related to apoptosis: possible implications for their mutagenic and carcinogenic effects, Toxicology 231 (2007) 159–174.
[15] J.Y. Ma, J.K. Ma, The dual effect of the particulate and organic components of diesel exhaust particles on the alteration of pulmonary immune/inflammatory responses and metabolic enzymes, J. Environ. Sci. Health C: Environ. Carcinog. Ecotoxicol. Rev. 20 (2002) 117–147.
[16] M. Castedo, J.L. Perfettini, T. Roumier, A. Valent, H. Raslova, K. Yakushijin, D. Horne, J. Feunteun, G. Lenoir, R. Medema, W. Vainchenker, G. Kroemer, Mitotic catastrophe constitutes a special case of apoptosis whose suppression entails aneuploidy, Oncogene 23 (2004) 4362–4370.
[17] S. Nowsheen, E.S. Yang, The intersection between DNA damage response and cell death pathways, Exp Oncol. 34 (2012) 243–254.
[18] G. Coster, M. Goldberg, The cellular response to DNA damage: a focus on MDC1 and its interacting proteins, Nucleus 1 (2010) 166–178.
[19] E.G. Seviour, S.Y. Lin, The DNA damage response: balancing the scale between cancer and ageing, Aging 2 (2010) 900–907.
[20] S. Ghosh, H. Narang, A. Sarma, H. Kaur, M. Krishna, Activation of DNA damage response signaling in lung adenocarcinoma A549 cells following oxygen beam irradiation, Mutat. Res. (2011).
[21] P.J. Hurley, F. Bunz, ATM and ATR: components of an integrated circuit, Cell Cycle 6 (2007) 414–417.
[22] Y. Kang, H.M. Cheong, J.H. Lee, P.I. Song, K.H. Lee, S.Y. Kim, J.Y. Jun, H.J. You, Protein phosphatase 5 is necessary for ATR-mediated DNA repair, Biochem. Biophys. Res. Commun. 404 (2011) 476–481.
[23] E. Strom, S. Sathe, P.G. Komarov, O.B. Chernova, I. Pavlovska, I. Shyshynova, D.A. Bosykh, L.G. Burdelya, R.M. Macklis, R. Skaliter, E.A. Komarova, A.V. Gudkov, Small-molecule inhibitor of p53 binding to mitochondria protects mice from gamma radiation, Nat. Chem. Biol. 2 (2006) 474–479.
[24] X.P. Zhang, F. Liu, W. Wang, Two-phase dynamics of p53 in the DNA damage response, Proc. Natl. Acad. Sci. U.S.A. (2011).
[25] R.C. Austin, The unfolded protein response in health and disease, Antioxid. Redox Signal. 11 (2009) 2279–2287.
[26] F. Osorio, B. Lambrecht, S. Janssens, The UPR and lung disease, Semin. Immunopathol. 35 (2013) 293–306.
[27] M. Kitamura, The unfolded protein response triggered by environmental factors, Semin Immunopathol. 35 (2013) 259–275.
[28] R. Mendez, Z. Zheng, Z. Fan, S. Rajagopalan, Q. Sun, K. Zhang, Exposure to fine airborne particulate matter induces macrophage infiltration, unfolded protein response, and lipid deposition in white adipose tissue, Am. J. Transl. Res. 5 (2013) 224–234.
[29] T.L. Watterson, B. Hamilton, R. Martin, R.A. Coulombe Jr., Urban particulate matter causes ER stress and the unfolded protein response in human lung cells, Toxicol. Sci. 112 (2009) 111–122.
[30] R. Sano, J.C. Reed, ER stress-induced cell death mechanisms, Biochim. Biophys. Acta (2013).
[31] H. Malhi, M.E. Guicciardi, G.J. Gores, Hepatocyte death: a clear and present danger, Physiol. Rev. 90 (2010) 1165–1194.
[32] A. Solhaug, S. Ovrebo, S. Mollerup, M. Lag, P.E. Schwarze, S. Nesnow, J.A. Holme, Role of cell signaling in B[a]P-induced apoptosis: characterization of unspecific effects of cell signaling inhibitors and apoptotic effects of B[a]P metabolites, Chem. Biol. Interact. 151 (2005) 101–119.
[33] A. Solhaug, M. Refsnes, J.A. Holme, Role of cell signalling involved in induction of apoptosis by benzo[a]pyrene and cyclopenta[c,d]pyrene in Hepa1c1c7 cells, J. Cell. Biochem. 93 (2004) 1143–1154.
[34] N. Asare, X. Tekpli, M. Rissel, A. Solhaug, N. Landvik, V. Lecureur, N. Podechard, G. Brunborg, M. Lag, D. Lagadic-Gossmann, J.A. Holme, Signalling pathways involved in 1-nitropyrene (1-NP)-induced and 3-nitrofluoranthene (3-NF)-induced cell death in Hepa1c1c7 cells, Mutagenesis 24 (2009) 481–493.
[35] E. Oya, J. Ovrevik, V.M. Arlt, E. Nagy, D.H. Phillips, J.A. Holme, DNA damage and DNA damage response in human bronchial epithelial BEAS-2B cells following exposure to 2-nitrobenzanthrone and 3-nitrobenzanthrone: role in apoptosis, Mutagenesis 26 (2011) 697–708.
[36] M. Gualtieri, J. Ovrevik, S. Mollerup, N. Asare, E. Longhin, H.J. Dahlman, M. Camatini, J.A. Holme, Airborne urban particles (Milan winter-PM2.5) cause mitotic arrest and cell death: effects on DNA, mitochondria, AhR binding and spindle organization, Mutat. Res. 713 (2011) 18–31.
[37] J. Ovrevik, V.M. Arlt, E. Oya, E. Nagy, S. Mollerup, D.H. Phillips, M. Lag, J.A. Holme, Differential effects of nitro-PAHs and amino-PAHs on cytokine and chemokine responses in human bronchial epithelial BEAS-2B cells, Toxicol. Appl. Pharmacol. 242 (2010) 270–280.
[38] J. Ovrevik, J.A. Holme, M. Lag, P.E. Schwarze, M. Refsnes, Differential chemokine induction by 1-nitropyrene and 1-aminopyrene in bronchial epithelial cells: importance of the TACE/TGF-alpha/EGFR-pathway, Environ. Toxicol. Pharmacol. 35 (2013) 235–239.
[39] J. Ovrevik, M. Refsnes, J.A. Holme, P.E. Schwarze, M. Lag, Mechanisms of chemokine responses by polycyclic aromatic hydrocarbons in bronchial epithelial cells: sensitization through toll-like receptor-3 priming, Toxicol. Lett. 219 (2013) 125–132.
[40] P.E. Schwarze, A.I. Totlandsdal, M. Lag, M. Refsnes, J.A. Holme, J. Ovrevik, Inflammation-related effects of diesel engine exhaust particles: studies on lung cells in vitro, Biomed. Res. Int. 2013 (2013) 685142.
[41] K. Imaida, M.S. Lee, C.Y. Wang, C.M. King, Carcinogenicity of dinitropyrenes in the weanling female CD rat, Carcinogenesis 12 (1991) 1187–1191.
[42] H. Ohgaki, C. Negishi, K. Wakabayashi, K. Kusama, S. Sato, T. Sugimura, Induction of sarcomas in rats by subcutaneous injection of dinitropyrenes, Carcinogenesis 5 (1984) 583–585.
[43] S.P. Hussain, P. Amstad, K. Raja, M. Sawyer, L. Hofseth, P.G. Shields, A. Hewer, D.H. Phillips, D. Ryberg, A. Haugen, C.C. Harris, Mutability of p53 hotspot codons to benzo(a)pyrene diol epoxide (BPDE) and the frequency of p53 mutations in nontumorous human lung, Cancer Res. 61 (2001) 6350–6355.
[44] R.R. Reddel, Y. Ke, B.I. Gerwin, M.G. McMenamin, J.F. Lechner, R.T. Su, D.E. Brash, J.B. Park, J.S. Rhim, C.C. Harris, Transformation of human bronchial epithelial cells by infection with SV40 or adenovirus-12 SV40 hybrid virus, or transfection via strontium phosphate coprecipitation with a plasmid containing SV40 early region genes, Cancer Res. 48 (1988) 1904–1909.
[45] Z. Darzynkiewicz, X. Huang, Analysis of cellular DNA content by flow cytometry, Curr. Protoc. Immunol. 5 (2004) 7 (Chapter 5).
[46] A. Gammelsrud, A. Solhaug, B. Dendele, W.J. Sandberg, L. Ivanova, A. Kocbach Bolling, D. Lagadic-Gossmann, M. Refsnes, R. Becher, G. Eriksen, J.A. Holme, Enniatin B-induced cell death and inflammatory responses in RAW 267.4 murine macrophages, Toxicol. Appl. Pharmacol. 261 (2012) 74–87.
[47] A. Solhaug, L.L. Vines, L. Ivanova, B. Spilsberg, J.A. Holme, J. Pestka, A. Collins, G.S. Eriksen, Mechanisms involved in alternariol-induced cell cycle arrest, Mutat. Res. 738-739 (2012) 1–11.
[48] S.H. Hansen, A.K. Olsen, E.J. Soderlund, G. Brunborg, In vitro investigations of glycidamide-induced DNA lesions in mouse male germ cells and in mouse and human lymphocytes, Mutat. Res. 696 (2010) 55–61.
[49] J.E. Kucab, D.H. Phillips, V.M. Arlt, Metabolic activation of diesel exhaust carcinogens in primary and immortalized human TP53 knock-in (Hupki) mouse embryo fibroblasts, Environ. Mol. Mutagen. 53 (2012) 207–217.

[50] D.H. Phillips, V.M. Arlt, The 32P-postlabeling assay for DNA adducts, Nat. Protoc. 2 (2007) 2772–2781.
[51] A. Collins, M. Dusinska, M. Franklin, M. Somorovska, H. Petrovska, S. Duthie, L. Fillion, M. Panayiotidis, K. Raslova, N. Vaughan, Comet assay in human biomonitoring studies: reliability, validation, and applications, Environ. Mol. Mutagen. 30 (1997) 139–146.
[52] J.S. Dickey, C.E. Redon, A.J. Nakamura, B.J. Baird, O.A. Sedelnikova, W.M. Bonner, H2AX: functional roles and potential applications, Chromosoma 118 (2009) 683–692.
[53] K.A. Boehme, C. Blattner, Regulation of p53 – insights into a complex process, Crit. Rev. Biochem. Mol. Biol. 44 (2009) 367–392.
[54] C.A. Brady, L.D. Attardi, p53 at a glance, J. Cell Sci. 123 (2010) 2527–2532.
[55] K. Oda, H. Arakawa, T. Tanaka, K. Matsuda, C. Tanikawa, T. Mori, H. Nishimori, K. Tamai, T. Tokino, Y. Nakamura, Y. Taya, p53AIP1, a potential mediator of p53-dependent apoptosis, and its regulation by Ser-46-phosphorylated p53, Cell 102 (2000) 849–862.
[56] M. Tampio, J. Loikkanen, P. Myllynen, A. Mertanen, K.H. Vahakangas, Benzo(a)pyrene increases phosphorylation of p53 at serine 392 in relation to p53 induction and cell death in MCF-7 cells, Toxicol. Lett. 178 (2008) 152–159.
[57] E.A. Komarova, N. Neznanov, P.G. Komarov, M.V. Chernov, K. Wang, A.V. Gudkov, p53 inhibitor pifithrin alpha can suppress heat shock and glucocorticoid signaling pathways, J. Biol. Chem. 278 (2003) 15465–15468.
[58] N.E. Landvik, V.M. Arlt, E. Nagy, A. Solhaug, X. Tekpli, H.H. Schmeiser, M. Refsnes, D.H. Phillips, D. Lagadic-Gossmann, J.A. Holme, 3-Nitrobenzanthrone and 3-aminobenzanthrone induce DNA damage and cell signalling in Hepa1c1c7 cells, Mutat. Res. 684 (2010) 11–23.
[59] J. Ovrevik, M. Refsnes, A.I. Totlandsdal, J.A. Holme, P.E. Schwarze, M. Lag, TACE/TGF-alpha/EGFR regulates CXCL8 in bronchial epithelial cells exposed to particulate matter components, Eur. Respir. J. 38 (2011) 1189–1199.
[60] J. Ovrevik, M. Refsnes, P. Schwarze, M. Lag, The ability of oxidative stress to mimic quartz-induced chemokine responses is lung cell line-dependent, Toxicol. Lett. 181 (2008) 75–80.
[61] A.I. Totlandsdal, M. Lag, E. Lilleaas, F. Cassee, P. Schwarze, Differential proinflammatory responses induced by diesel exhaust particles with contrasting PAH and metal content, Environ. Toxicol. (2013).
[62] C. Garcia-Canton, E. Minet, A. Anadon, C. Meredith, Metabolic characterization of cell systems used in in vitro toxicology testing: lung cell system BEAS-2B as a working example, Toxicol. In Vitro 27 (2013) 1719–1727.
[63] C. Lepers, V. Andre, M. Dergham, S. Billet, A. Verdin, G. Garcon, D. Dewaele, F. Cazier, F. Sichel, P. Shirali, Xenobiotic metabolism induction and bulky DNA adducts generated by particulate matter pollution in BEAS-2B cell line: geographical and seasonal influence, J. Appl. Toxicol. (2013).
[64] A. Solhaug, M. Refsnes, M. Lag, P.E. Schwarze, T. Husoy, J.A. Holme, Polycyclic aromatic hydrocarbons induce both apoptotic and anti-apoptotic signals in Hepa1c1c7 cells, Carcinogenesis 25 (2004) 809–819.
[65] N. Podechard, X. Tekpli, D. Catheline, J.A. Holme, V. Rioux, P. Legrand, M. Rialland, O. Fardel, D. Lagadic-Gossmann, V. Lecureur, Mechanisms involved in lipid accumulation and apoptosis induced by 1-nitropyrene in Hepa1c1c7 cells, Toxicol. Lett. 206 (2011) 289–299.
[66] M. Leist, B. Single, A.F. Castoldi, S. Kuhnle, P. Nicotera, Intracellular adenosine triphosphate (ATP) concentration: a switch in the decision between apoptosis and necrosis, J. Exp. Med. 185 (1997) 1481–1486.
[67] P. Nicotera, M. Leist, E. Ferrando-May, Apoptosis and necrosis: different execution of the same death, Biochem. Soc. Symp. 66 (1999) 69–73.
[68] H. Yamazaki, N. Hatanaka, R. Kizu, K. Hayakawa, N. Shimada, F.P. Guengerich, M. Nakajima, T. Yokoi, Bioactivation of diesel exhaust particle extracts and their major nitrated polycyclic aromatic hydrocarbon components, 1-nitropyrene and dinitropyrenes, by human cytochromes P450 1A1, 1A2, and 1B1, Mutat. Res. 472 (2000) 129–138.
[69] E.P. Eddy, E.C. McCoy, H.S. Rosenkranz, R. Mermelstein, Dichotomy in the mutagenicity and genotoxicity of nitropyrenes: apparent effect of the number of electrons involved in nitroreduction, Mutat. Res. 161 (1986) 109–111.
[70] M. Stiborova, V. Martinek, M. Svobodova, J. Sistkova, Z. Dvorak, J. Ulrichova, V. Simanek, E. Frei, H.H. Schmeiser, D.H. Phillips, V.M. Arlt, Mechanisms of the different DNA adduct forming potentials of the urban air pollutants 2-nitrobenzanthrone and carcinogenic 3-nitrobenzanthrone, Chem. Res. Toxicol. 23 (2010) 1192–1201.
[71] J. Han, S.H. Back, J. Hur, Y.H. Lin, R. Gildersleeve, J. Shan, C.L. Yuan, D. Krokowski, S. Wang, M. Hatzoglou, M.S. Kilberg, M.A. Sartor, R.J. Kaufman, ER-stress-induced transcriptional regulation increases protein synthesis leading to cell death, Nat. Cell Biol. 15 (2013) 481–490.
[72] U. Rannug, J.A. Holme, J.K. Hongslo, R. Sram, International Commission for Protection against Environmental Mutagens and Carcinogens. An evaluation of the genetic toxicity of paracetamol, Mutat. Res. 327 (1995) 179–200.